vs. pH profile (zero buffer) in Figure 2 in the pH region from 7.5 to 8.0, i.e., that for rate-limiting attack of OH^- on the oxocarbonium ion.

At pH >10 the ring opening reaction becomes independent of pH. Similar pH-independent reactions have been found in the hydrolysis of acetals and ketals subject to general acid catalysis.[7,8,10] These reactions involve rate-determining unimolecular C–O bond breaking.[8] Thus the analogous reaction of II may also involve a unimolecular decomposition (VIII). Such a reaction would be

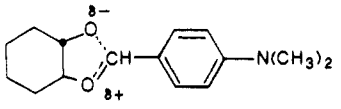

VIII

due to the significant oxocarbonium ion stabilization and the ease of C–O bond breaking brought about by relief of steric strain in the acetal of *trans*-1,2-cyclohexanediol. An alternative possibility is that water is acting as a general acid, which would require a second-order rate constant of 1.1×10^{-6} M^{-1} s^{-1} (k_o/55.5 M). This second-order rate constant fits reasonably well on a Brønsted plot of slope –0.7 including points for the general acids and hydronium ion.

In summary, in the plot of log k_{obsd} vs. pH for the hydrolysis of *trans*-1,2-cyclohexanediol *p*-(dimethylamino)benzylidene acetal in H_2O there are seven inflections, only one of which is due to an ionizable group (the *p*-dimethylamino group conjugate acid). As discussed, the other inflections are produced by two changes in rate-determining step and four changes in mechanism as pH is increased. This novel situation comes about because of steric strain in the acetal, so that ring opening is rapid, and the cyclic structure of the acetal, which can lead to reversibility of ring opening. The resultant compromise between these opposing factors is one in which each step becomes rate limiting in turn as pH is increased. Hemiacetal breakdown can only be rate determining at pH <6 because of OH^- catalysis at higher pH. Rate-limiting hydrolysis of the protonated and neutral species of the hemiacetal at low pH is brought about because of the rapid hydronium ion catalyzed ring opening or $k_{-2}a_H > k_3$. As the pH is increased above 6 attack of a water molecule on the oxocarbonium ion intermediate becomes rate limiting because at those pH values the hydroxide ion catalyzed breakdown of the hemiacetal is rapid with $k_3(OH^-) > k_{-2}a_H$. The mechanism changes at pH >7 to attack of OH^- on the oxocarbonium ion, and as the concentration of OH^- becomes larger the hydronium ion catalyzed ring opening becomes rate determining, i.e., $k_{OH}(OH^-) > k_{-1}$. The ring-opening is also catalyzed by general acids. Finally at pH >10 the mechanism changes to pH-independent rate-determining ring opening. Thus, *all* of the mechanisms and rate-determining steps for the hydrolysis of an acetal are represented on one remarkable log k_{obsd} vs. pH profile (Figure 2).

Acknowledgment. This work was supported by a research grant from the National Institutes of Health.

Registry No. I, 103457-39-2; II, 103457-40-5; III, 41564-26-5; IV, 24148-95-6.

Structure Elucidation of the Antibiotic Desertomycin through the Use of New Two-Dimensional NMR Techniques

Ad Bax,*† A. Aszalos,‡ Z. Dinya,§ and K. Sudo‡⊥

Contribution from the Laboratory of Chemical Physics, National Institute of Arthritis, Diabetes, and Digestive and Kidney Diseases, National Institutes of Health, Bethesda, Maryland 20892, the Division of Drug Biology, Food and Drug Administration, Washington, D.C. 20204, and the Antibiotics Research Laboratory, Kossuth University, Debrecen, Hungary.
Received March 20, 1986

Abstract: The structure of the antibiotic desertomycin has been determined by using modern two-dimensional NMR techniques. Mass spectroscopy indicated a M_r of 1192. All other structural information was obtained from ^1H and ^{13}C NMR. ^1H–^1H double-quantum-filtered COSY and homonuclear Hartmann–Hahn spectroscopy in combination with heteronuclear shift correlation and ^1H-detected heteronuclear multiple-bond multiple-quantum coherence were used for obtaining all crucial connectivities required for establishing the structure. Complete ^1H and ^{13}C assignments are also presented. The apparent molecular formula of desertomycin was determined as $C_{61}H_{109}NO_{21}$.

Isolation of desertomycin, a broad-spectrum antibiotic, was reported first by Uri et al.[1] in 1958. Preliminary structural work indicated the presence of a mannose moiety in the antibiotic.[2] Some physicochemical characteristics and a (erroneous) molecular formula of $C_{57}H_{109}NO_{24}$ were reported by Dolak et al.[3] in 1983. Interesting biological properties of desertomycin such as blockage of K^+ channels in muscle fibers,[4] selective isolation of human pathogenic fungi in culture,[5] and cytotoxicity against leukemia cells[6] also have been reported. Because of these interesting properties, we have undertaken the structure elucidation of desertomycin. Repeated initial attempts to grow crystals suitable for X-ray diffraction studies failed, forcing us to use the newer types of NMR techniques for determining the structure. As will be demonstrated here, when the new techniques are used on a high-field NMR spectrometer, they provide surprisingly simple and unambiguous means for determining the structure of molecules the size of desertomycin.

† Laboratory of Chemical Physics, National Institute of Arthritis, Diabetes, and Digestive and Kidney Diseases.
‡ Division of Drug Biology, Food and Drug Administration.
§ Antibiotics Research Laboratory.
⊥ Present address: Daiichi Seiyaku Co., Tokyo, Japan.

(1) Uri, J.; Bognar, R.; Bekesi, I.; Varga, B. *Nature (London)* **1958**, *182*, 401.
(2) Bognar, R.; Sztaricskai, F.; Somogyi, L.; Puskas, M.; Makleit, S. *Acta Chim. Acad. Sci. Hung.* **1968**, *56*, 53.
(3) Dolak, L. A.; Reusser, F.; Baczynskyj, L.; Mizsak, S. A.; Hannon, B. R.; Castle, T. M. *J. Antibiot.* **1983**, *36*, 13.
(4) Keresztes, T.; Gesztelyi, I.; Bekesi, I.; Korver, A. *Magy. Tud. Akad. Biol. Tud. Oszt. Kozl.* **1982**, *25*, 169.
(5) Uri, J.; Herpay, Zs. *Mykosen* **1961**, *4*, 128.
(6) Valy-Nagy, T.; Hernady, F.; Szabo, G.; Jeney, A. *Antibiot. Chemother. (Washington, D.C.)* **1961**, *11*, 238.

0002-7863/86/1508-8056$01.50/0

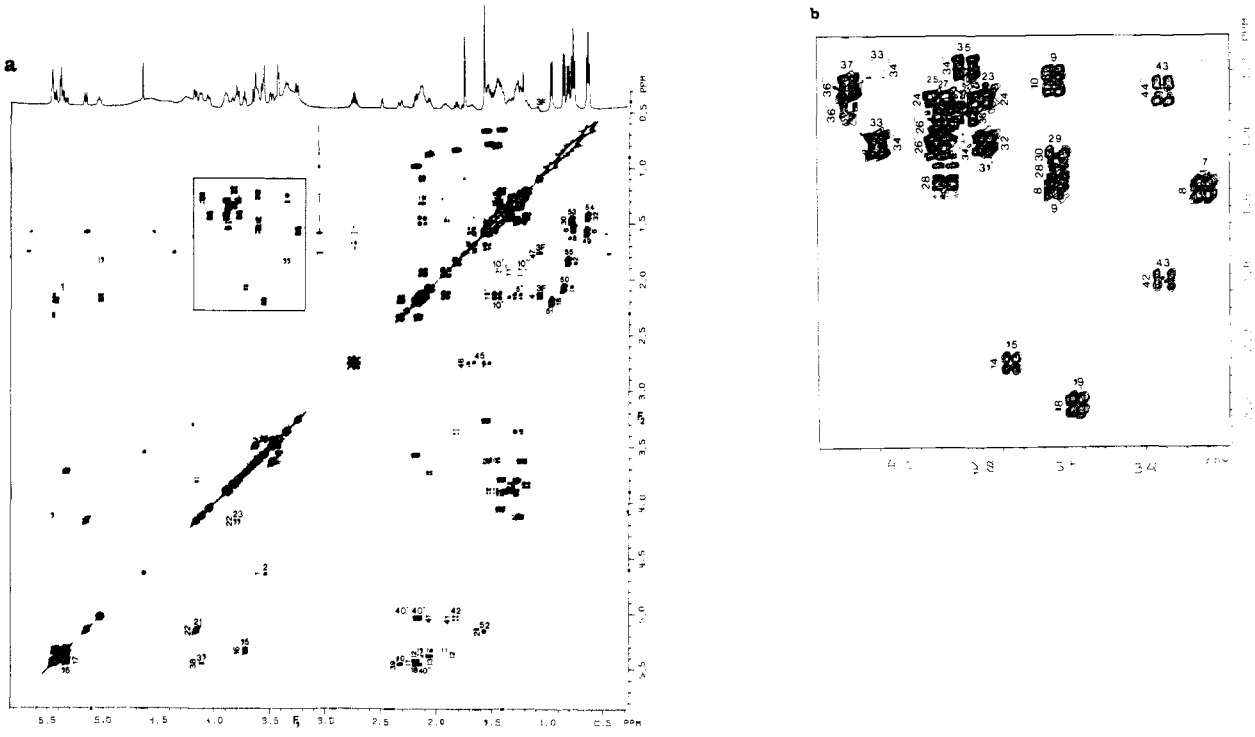

Figure 1. (a) Two-dimensional double-quantum-filtered COSY spectrum of desertomycin, with the conventional 1D ^1H spectrum shown along the top axis. Both positive and negative resonances are displayed. The C3H resonance (6.64 ppm) is folded and appears at 1.10 ppm. (b) Enlargement of the boxed region in a.

The approach used for determining the structure involves (a) ^1H–^1H double-quantum-filtered phase-sensitive COSY,[7-9] (b) homonuclear Hartmann–Hahn (HOHAHA) experiments,[9-13] (c) correlation of proton and ^{13}C chemical shifts,[14-18] and (d) ^1H-detected heteronuclear multiple-bond ^1H–^{13}C correlation (HMBC).[19,20] Both 2D NOE spectroscopy[21] and ^1H-detected ^1H–^{13}C correlation spectroscopy[22] are used for determining the stereochemistry about the double bonds.

Experimental Approach

First, all experiments used for the structure determination will be discussed. A detailed analysis of the corresponding NMR spectra is deferred to the second part of this paper.

Determining the structure of desertomycin by means of NMR presents problems that usually are not encountered in the study of smaller molecules. First, the ^1H spectrum shows a large amount of overlap, especially in the methylene region but also in the olefinic region and in the 3.4–3.8 ppm region (Figure 1). Second, for desertomycin, dimethyl sulfoxide had to be used as a solvent. In methanol, the presence of more than one conformational isomer complicates the NMR spectrum. The use of dimethyl sulfoxide as a solvent resulted in rather slow tumbling of the molecule and consequent line broadening of the ^1H and ^{13}C resonances. To minimize this effect all experiments were carried out at 55 °C, resulting in natural ^1H and ^{13}C line widths that vary from about 2 to 5 Hz.[23] The NMR approach requires determination of the complete proton-coupling network together with assignment of the resonances of all carbons coupled to these protons. Together with knowledge of the molecular weight and identification of the positions of nonprotonated carbons and heteroatoms in the molecular skeleton, this provides sufficient information to define the structure.

The first step involves the recording of a phase-sensitive double-quantum-filtered COSY spectrum.[7-9] This method yields antiphase absorption mode line shapes for the cross peaks and near-absorption antiphase line shapes for the components of diagonal multiplets. It is generally accepted that this method can offer a substantial improvement in resolution compared to the conventional absolute value mode method.[24,25] The COSY spectrum resulting from a 14-h accumulation is presented in Figure 1. The large amount of overlap among cross peaks present in this spectrum (especially when presented at a lower contour level) makes determining the entire ^1H-coupling network impossible. Moreover, some pairs of vicinally coupled protons have vanishingly low cross-peaks intensities because of small couplings and large natural line widths.

To obtain more information about ^1H–^1H scalar connectivity, the recently developed HOHAHA experiment[9-13] was used to determine relayed connectivity. This method yields high-resolution near-absorptive 2D spectra that display cross peaks among protons that are separated by more than three bonds. Unfortunately, in

(7) Rance, M.; Sorensen, O. W.; Bodenhausen, G.; Wagner, G.; Ernst, R. R.; Wuthrich, K. *Biochem. Biophys. Res. Commun.* **1983**, *117*, 479.
(8) Marion, D.; Wuthrich, K. *Biochem. Biophys. Res. Commun.* **1983**, *113*, 967.
(9) Edwards, M. W.; Bax, A. *J. Am. Chem. Soc.* **1986**, *108*, 918–923.
(10) Braunschweiler, L.; Ernst, R. R. *J. Magn. Reson.* **1983**, *53*, 521.
(11) Davis, D. G.; Bax, A. *J. Am. Chem. Soc.* **1985**, *107*, 2820.
(12) Bax, A.; Davis, D. G. *J. Magn. Reson.* **1985**, *65*, 355.
(13) Bax, A.; Davis, D. G. In *Advanced Magnetic Resonance Techniques in Systems of High Molecular Complexity*; Nicolai, N., Valensin, G., Eds.; Birkhauser: Basel, in press.
(14) Maudsley, A. A.; Muller, L.; Ernst, R. R. *J. Magn. Reson.* **1977**, *28*, 463.
(15) Bodenhausen, G.; Freeman, R. *J. Magn. Reson.* **1977**, *28*, 471.
(16) Bax, A.; Morris, G. A. *J. Magn. Reson.* **1981**, *42*, 501.
(17) Bax, A. In *Topics in Carbon-13 NMR*; Levy, G. C., Ed.; Wiley: New York, 1984; Vol. 4, Chapter 8.
(18) Bax, A.; Sarkar, S. K. *J. Magn. Reson.* **1984**, *60*, 170.
(19) Bax, A.; Summers, M. F. *J. Am. Chem. Soc.* **1986**, *108*, 2093.
(20) Summers, M. F.; Marzilli, L. G.; Bax, A. *J. Am. Chem. Soc.* **1986**, *108*, 4285.
(21) Jeener, J.; Meier, B. H.; Ernst, R. R. *J. Chem. Phys.* **1979**, *71*, 4546.
(22) Bax, A.; Subramanian, S. *J. Magn. Reson.* **1986**, *67*, 565.
(23) ^1H T_2's were measured with a 90°–τ–180°–τ-acq sequence, using a weak radio frequency field of 100 Hz (2.5-ms, 90° pulse width). T_2 values ranged from 75 to 150 ms. ^{13}C T_2 values were measured by using a similar spin–echo sequence with nonselective pulses and no ^1H decoupling during the τ periods. ^{13}C T_2 values ranged from about 200 ms for the nonprotonated olefinic carbons to 60 ms for the methylene carbons.
(24) Aue, W. P.; Bartholdi, E.; Ernst, R. R. *J. Chem. Phys.* **1976**, *64*, 2229.
(25) Bax, A.; Freeman, R. *J. Magn. Reson.* **1981**, *44*, 542.

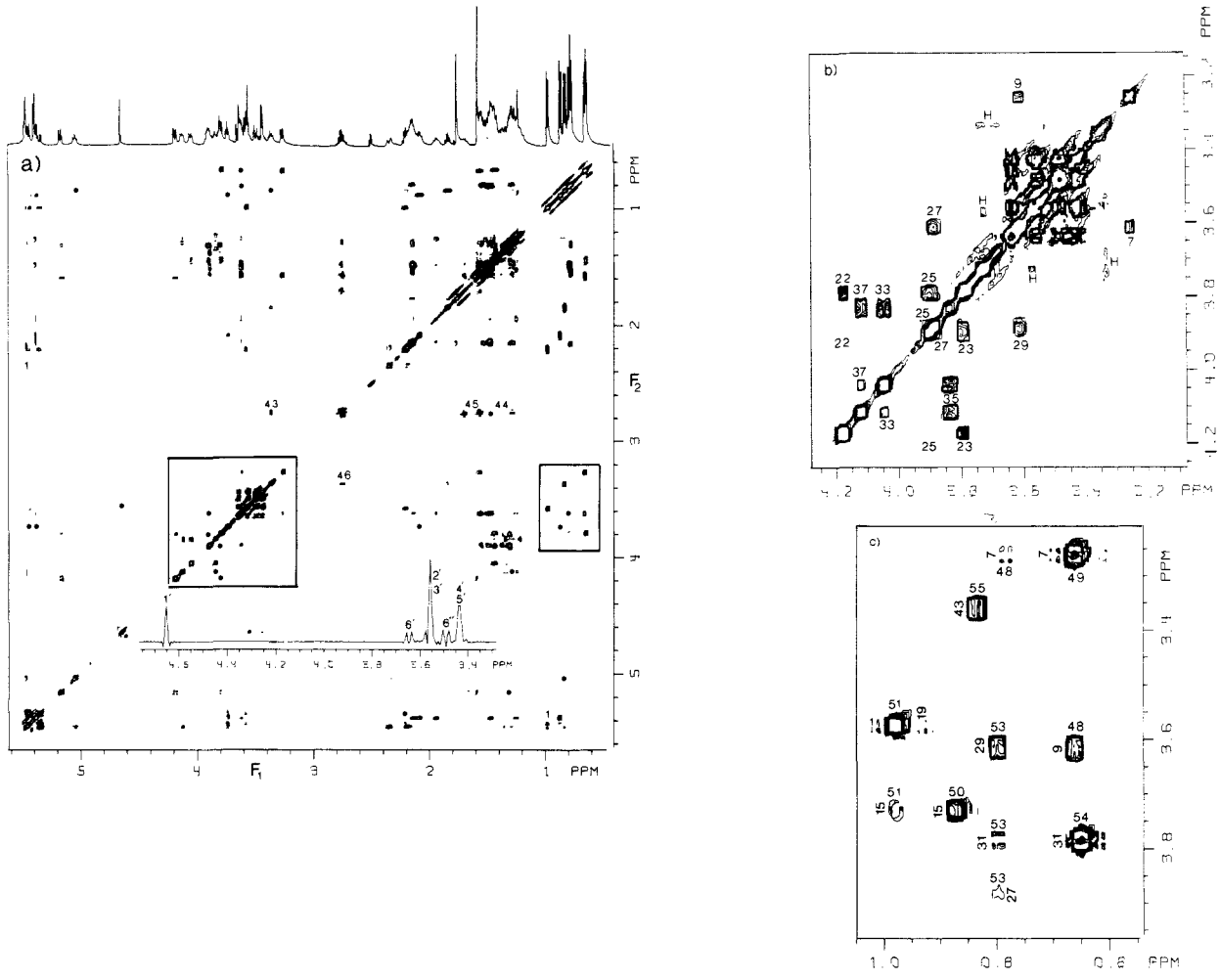

Figure 2. (a) Two-dimensional phase-sensitive HOHAHA spectrum showing direct and relayed $^1H-^1H$ connectivity. Spinning sidebands near the diagonal are visible for intense methyl resonances. The inset is part of an F_1 cross section, taken at $F_2 = 3.55$ ppm, and shows all the mannose resonances. (b and c) Enlargements of the boxed regions in a, displayed at lower contour levels. Resonances from hydroxyl protons that have not been exchanged with deuterons are marked "H". The intense correlations $C49H_3/C7H$, $C51H_3/C19H$, and $C54H_3/C31H$ show some truncation artifacts when displayed at low contour levels (c).

the HOHAHA experiment chemical exchange gives rise to cross peaks that are virtually indistinguishable from Hartmann–Hahn cross peaks.[26] Because the hydroxyl protons (in the 3–5 ppm region) are in slow chemical exchange, the corresponding region in the HOHAHA spectrum recorded originally was intractable. Therefore, the hydroxyl protons were exchanged with deuterons, resulting in a 2D spectrum almost completely free of exchange peaks. For this spectrum, displayed in Figure 2, an 80-ms mixing time was used, and cross peaks between protons up to six bonds apart are present in this spectrum.

Of course, ^{13}C NMR presents an important additional tool for structure determination. The number of protons coupled to a particular carbon can be determined easily by the use of spectral editing experiments. Moreover, ^{13}C chemical shifts are far more sensitive to their chemical environment than proton shifts, presenting valuable structural information. An absorption mode 2D heteronuclear shift correlation spectrum is presented in Figure 3. The corresponding 1D ^{13}C spectrum is shown along the F_2 axis of this spectrum. The resonance of the anomeric mannose carbon (96.0 ppm) and a carbonyl resonance (166.4 ppm) are also present in the 1D spectrum but are not shown. The spectrum of Figure 3 was recorded for 120 mg of material dissolved in 3 mL of solvent and required a 12-h measuring time. The refocused INEPT experiment[27] was used for distinguishing methylene and methine carbons (spectrum not shown). Several attempts were made to record a $^1H-^1H-^{13}C$ RELAY spectrum[28,29] but the signal-to-noise ratio of the resulting spectra (using a 120-mg sample) was too low to yield useful information.

None of the experiments described above presents unambiguous information about the three nonprotonated carbons detected in the 1D ^{13}C spectrum. Also, as will be discussed later, despite use of the double-quantum-filtered COSY and HOHAHA experiments, a number of $^1H-^1H$ connectivities could not be established unequivocally. Both problems were solved by using the recently proposed ^1H-detected heteronuclear multiple-bond correlation (HMBC) method.[19] A detailed discussion of the optimization of this new technique is given by Summers et al.[20] To cover the entire ^{13}C spectral width, two experiments were performed with the ^{13}C carrier positioned at 55 and 145 ppm, respectively. The corresponding spectra are shown in Figure 4. The large number of long-range connectivities visible in these spectra is particularly impressive considering that only 16 mg of sample was used and that the $^1H-^{13}C$ long-range couplings that give rise to a detectable connectivity (typically 3–5 Hz) are of the same order of magnitude as the natural line widths of the ^1H and ^{13}C resonances. The combination of all the connectivities present in the spectra of Figures 1–4 presents ample information for determining an unambiguous primary structure of desertomycin.

Determination of the stereochemistry about the double bonds present in desertomycin was made by measurement of the $^3J_{HH}$

(26) Davis, D. G.; Bax, A. *J. Magn. Reson.* **1985**, *64*, 533.
(27) Burum, D. P.; Ernst, R. R. *J. magn. Reson.* **1980**, *39*, 163.
(28) Bolton, P. H. *J. Magn. Reson.* **1982**, *48*, 336. Kessler, H.; Bernd, M.; Kogler, H.; Zarbock, J.; Sorensen, O. W.; Bodenhausen, G.; Ernst, R. R. *J. Am. Chem. Soc.* **1983**, *105*, 6944.
(29) Bax, A.; Davis, D. G.; Sarkar, S. K. *J. Magn. Reson.* **1985**, *63*, 230.

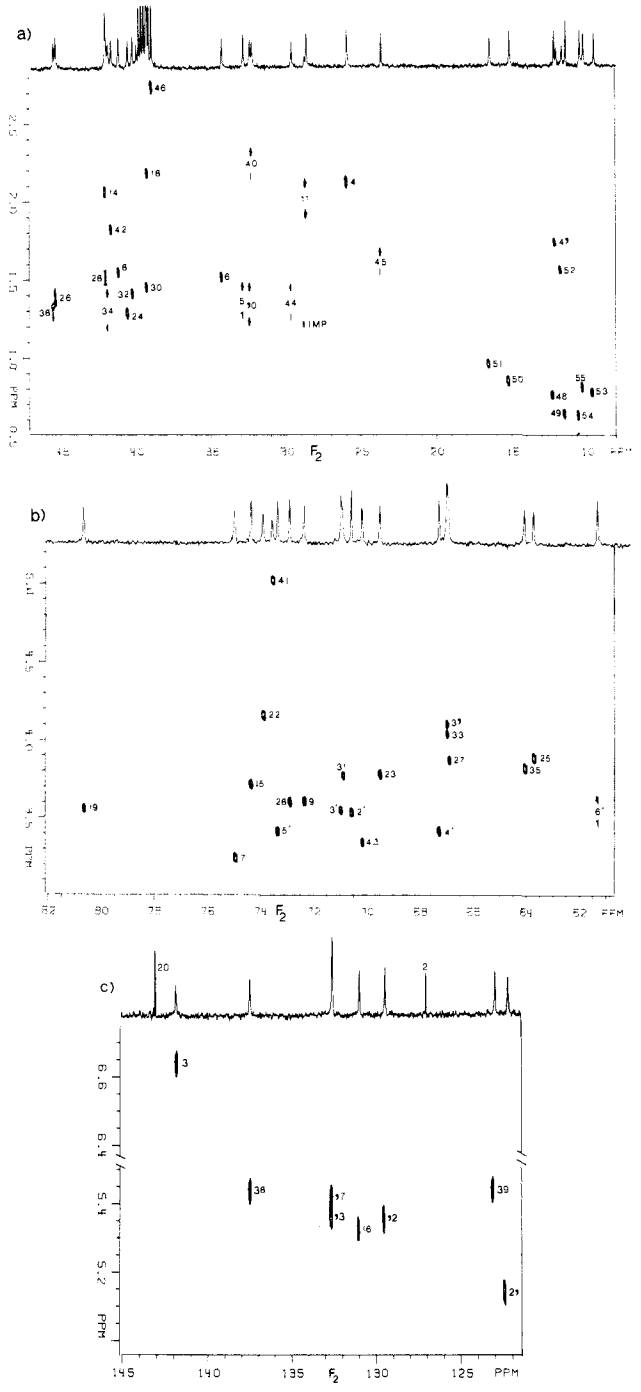

Figure 3. Three regions of the absorption mode $^1H-^{13}C$ shift correlation spectrum, displaying connectivity via one-bond J_{CH} coupling.

coupling, using the well-known fact that trans couplings via an olefinic bond are substantially larger than cis couplings. Because two pairs of coupled olefinic protons have nearly identical chemical shifts, the coupling constants for these protons were measured from the ^1H-detected $^1H-^{13}C$ shift correlation spectrum,[22] without ^{13}C decoupling during ^1H data acquisition (Figure 5). This spectrum results from a 3-h experiment, using 16 mg of sample. Resolution enhancement in the ^1H dimension of the 2D spectrum was used to facilitate accurate measurements of the J_{HH} couplings from the spectrum. Despite the fact that the intensity of a ^{13}C resonance in this spectrum is spread over two multiplets, separated by $^1J_{CH}$, each showing a number of well-resolved homonuclear couplings, the sensitivity is more than sufficient to measure the size of the vicinal olefinic proton couplings. As will be shown below, two of the olefinic bonds in desertomycin carry a methyl substituent. For these double bonds, the stereochemistry has been determined by 2D NOE spectroscopy (data not shown).

Chart I

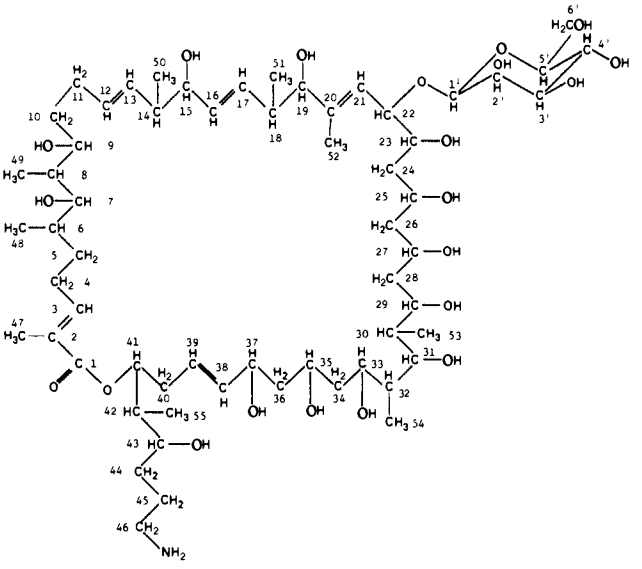

Results

The following discussion of the structure determination of desertomycin will rely mainly on the long-range $^1H-^{13}C$ connectivity spectra (Figure 4) because very few of the correlations in these spectra show overlap. The desertomycin structure we propose is shown in Chart I. The ^1H and ^{13}C chemical shifts and the $^1H-^{13}C$ multiple-bond connectivities are presented in Table I.

Starting at the most downfield proton (C3H [the proton on the C3 carbon] at 6.65 ppm), connectivity is observed in Figure 4b to a carbonyl (C1 at 166.5 ppm) and a nonprotonated olefinic carbon (C2 at 127 ppm) and in Figure 4a to a methyl carbon (C47 at 12.0 ppm) and two methylene carbons at 25.9 (C4) and 32.9 (C5) ppm. The 6.65 ppm proton is directly attached to an olefinic carbon (C3) at 141.8 ppm (Figure 3c). Also, Figure 4b shows connectivity between methyl protons $C47H_3$ (identified by correlation with C47 in Figure 3) and carbons C1, C2, and C3. Proton C3H (folded and appearing at 1.10 ppm in Figure 1a) shows a cross peak in the COSY spectrum with a resonance at 2.15 ppm, corresponding to two protons ($C4H_2$) that are both coupled to the same carbon at 25.9 ppm (Figure 3a). The refocused INEPT experiment (data not shown) confirmed that the carbon at 25.9 ppm is indeed of the methylene type. C5 (at 32.9 ppm) has two protons attached that resonate at 1.47 and 1.28 ppm. In the case of two nonequivalent methylene protons, we will refer to the proton resonating furthest downfield as H′ and to the other one as H″. Cross peaks between $C4H_2$ and C5H′ and C5H″ are present, but because both the C4 and the C5 protons overlap with other protons, this information alone would be insufficient for determining the connectivity between these protons. On the basis of the above evidence, one can construct the first part of the molecule, from carbon C1 to C5.

Methyl protons $C48H_3$ are coupled to carbon C5 and also show connectivity to a methine carbon at 34.3 ppm (C6) and a carbon at 74.9 ppm (C7) (Figure 4a). The chemical shift of C7 suggests a hydroxyl group is attached to it.

The presence of methyl groups is particularly helpful when using the HMBC method because three methyl protons are used to detect the presence of a carbon atom, enhancing the sensitivity of the method by a factor of 3. Moreover, couplings between methyl protons and carbons that are two or three bonds removed are generally quite large[30] (3.5–5 Hz), and methyl proton multiplets show relatively little homonuclear splittings (all doublets or singlets in desertomycin). For a wide variety of compounds studied with the HMBC method so far, invariably we have detected the connectivity to all the carbons two and three bonds

(30) Hansen, P. E. *Prog. Nucl. Magn. Reson. Spectrosc.* **1981**, *14*, 175.

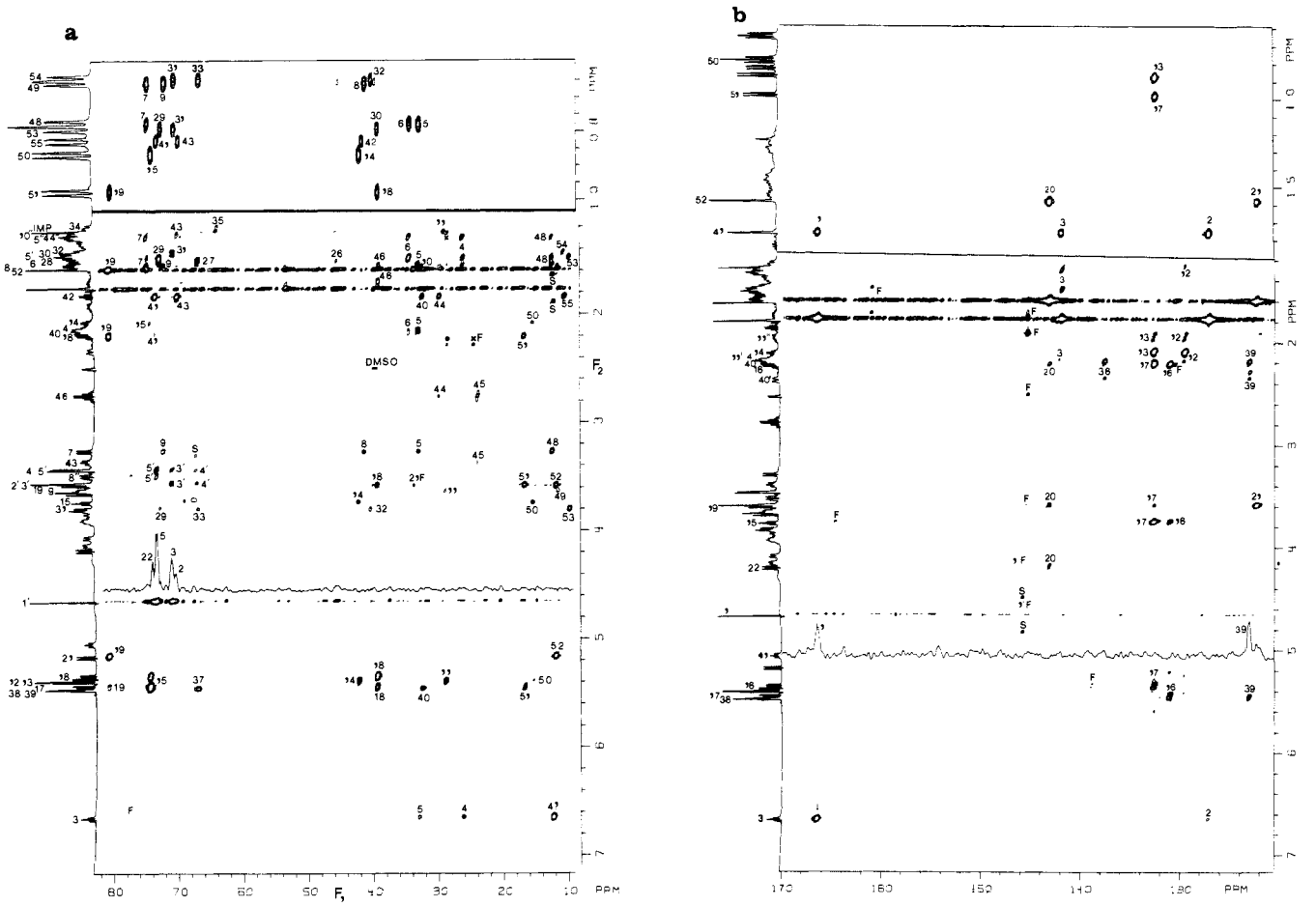

Figure 4. Absolute value mode representation of heteronuclear multipe-bond correlation spectra of (a) the high-field ^{13}C region and (b) the low-field ^{13}C region. The two spectra result from separate experiments and show two- and three-bond $^{1}H-^{13}C$ connectivity. The lowest contour level for correlations to the methyl protons (above the solid lines) is 5 times higher than for the remaining part of the spectra. Incompletely suppressed signals from one-bond correlations (displaced by $\pm^{1}J_{CH}/2$ in the F_2 dimension) are indicated by "S". Correlations from a small amount of impurity are marked "x". Resonances folded in the F_1 dimension are marked "F". In the ^{1}H spectrum, shown along the F_2 axis of the 2D spectra, resonances of the sugar protons in the 4.65–3.4 ppm region are labeled 1′–6′ and 6″. For resonances upfield from 3.4 ppm, H′ and H″ refer to nonequivalent geminal protons; the proton resonating furthest downfield is labeled H′.

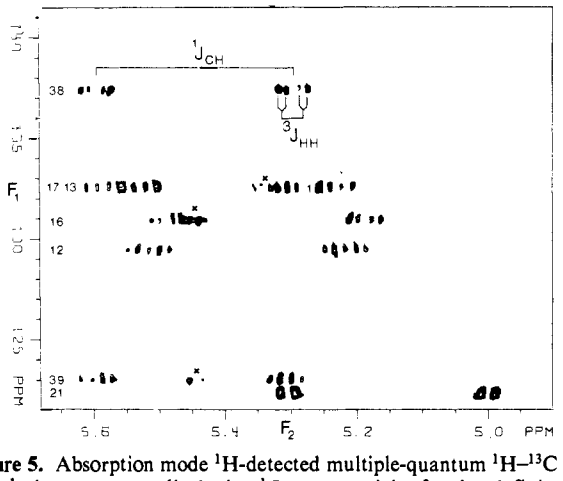

Figure 5. Absorption mode ^{1}H-detected multiple-quantum $^{1}H-^{13}C$ shift correlation spectrum, displaying $^{1}J_{CH}$ connectivity for the olefinic resonances. No ^{13}C decoupling was used during ^{1}H data acquisition, and line narrowing in the ^{1}H dimension was used to facilitate the measurement of the vicinal J_{HH} couplings. Correlations due to multiple-bond $^{1}J_{CH}$ couplings are marked "x".

removed from the methyl protons. The coupling between C7H and C6H is small (2 Hz), corresponding to a dihedral angle near 90°, and no C6H/C7H cross peak is visible in the COSY spectrum. In the HOHAHA spectrum, however, a small C7H/C48H_3 cross peak is present (Figure 2c), confirming the HMBC data. Protons C49H_3 show coupling to carbons C7, C8, and C9 (Figure 4a). C8H (1.57 ppm) shows connectivity to C10 (32.4 ppm), but this correlation is partially obscured by the t_1 noise of methyl protons C52H_3 (1.58 ppm) and by an intense correlation between C6H and C5 (Figure 4a). Also, in the COSY spectrum (Figure 1b), a cross peak between C9H and C10H″ (identified by correlation with C9 and C10, respectively) confirms this connectivity. C9H shows coupling to a carbon at 28.6 ppm (Figure 4a), which is then labeled C11. Of the two protons coupled to C11, the upfield proton C11H″ shows coupling to both C10H′ and C10H″ (Figure 1a), confirming the HMBC data.

The next 12 carbons in the chain are identified relatively easily. C11H″ is coupled to olefinic carbons at 129.4 and 132.6 ppm (Figure 4b), which are then labeled C12 and C13. Both C12 and C13 are coupled to protons at 5.38 ppm (Figure 3c), and it is not immediately clear what is the correct ^{13}C assignment of these two carbons. The carbon at 132.6 ppm is coupled to methyl protons at 0.87 ppm (C5OH_3), which then assigns this resonance to C13. Both C12 and C13 are also coupled to a proton at 2.10 ppm (Figure 4b), which is then labeled C14H. The C14 carbon resonance is identified from Figure 3a, and as expected, methyl protons C50H_3 are coupled to this carbon (Figure 4a). Protons C50H_3 are also coupled to a carbon at 74.3 ppm, labeled C15, which has a directly attached proton at 3.73 ppm. Figure 1b shows that C15H is coupled to C14H and (Figure 1a) to an olefinic proton at 5.35 ppm (C16H) which is coupled to a proton at 5.44 ppm (C17H). Corresponding carbons C16 and C17 resonate at 130.9 and 132.6 ppm, respectively (Figure 3c, Figure 5). The HMBC spectrum also shows connectivity between C15H and C16 and C17 (Figure 4b). C17H shows connectivity to a proton at 2.19 ppm, labeled C18H, which is coupled to methyl protons C51H_3. These observations are confirmed by connectivity in

Table I. ^1H and ^{13}C Chemical Shift Assignments (ppm) for Desertomycin and Protons to Which a Long-Range Connectivity Is Observed in the HMBC Experiment

assignment	^{13}C	^1H	HMBC (^1H)
53	9.57	0.80	C31H, C30H
55	10.21	0.83	C41H,[b] C43H,[b] C42H
54	10.46	0.64	C33H,[b] C32H
49	11.39	0.66	C8H, C9H
52	11.66	1.58	C21H, C19H
47	12.03	1.77	C3H
48	12.17	0.78	C7H, C5H′, C5H″, C6H
50	15.13	0.87	C13H, C14H,[b] C15H
51	16.44	0.98	C17H, C18H, C19H
45	23.67	1.57, 1.71	C43H, $C46H_2$
4	25.94	2.15	C3H, C5H′, C5H″, C6H
11	28.64	1.95, 2.14	C12H/C13H,[a] C9H, C10H″
44	29.64	1.28, 1.47	$C46H_2$, C42H,[b] C43H, C45H″,[b]
40	32.28	2.18, 2.33	C38H/C39H,[a] C42H[b]
10	32.42	1.24, 1.48	C8H
5	32.85	1.28, 1.47	$C48H_3$, C3H, C7H, C4H, C6H
6	34.28	1.53	$C48H_3$, C4H, C5H′, C5H″
46	39.0	2.75	C44H″,[b] C45H′, C45H″
18	39.17	2.21	$C51H_3$, C16H, C17H, C19H
30	39.33	1.47	$C53H_3$
32	40.26	1.44	$C54H_3$, C31H
24	40.57	1.28	C22H[b]
8	41.18	1.57	$C49H_3$, C7H
42	41.68	1.83	$C55H_3$
34	41.89	1.22, 1.44	
14	42.06	2.10	$C50H_3$, C12H/C13H,[a] C15H
28	42.06	1.55, 1.51	C30H[b]
26	45.38	1.43, 1.38	C28H′,[b] C28H″
36	45.52	1.27, 1.34	
6′	61.26	3.49, 3.63	
25	63.67	3.90	C24H[b]
35	64.01	3.83	C33H,[b] C34H″
27	66.85	3.88	C26H′,[b] C28H″
33	66.94	4.05	$C54H_3$, C31H
37	66.94	4.12	C38H/C39H[a]
4′	67.24	3.42	C5′H, C3′H
23	69.46	3.80	C22H,[b] C24H′,[b] C24H″[b]
43	70.13	3.35	$C55H_3$, C42H, C44H″
2′	70.53	3.54	C1′H
31	70.91	3.79	$C54H_3$, $C53H_3$, C33H,[b] C32H
3′	71.01	3.55	C1′H, C4′H/C5′H,[a] C2′H
9	72.31	3.61	$C49H_3$, C7H, C8H
29	72.85	3.61	$C53H_3$, C28H″,[b] C30H[b] C31H
5′	73.30	3.42	C1′H, C4′H, C6′H″
41	73.50	5.05	$C55H_3$, C40H″,[b] C42H
22	73.85	4.17	C1′H
15	74.30	3.73	C16H, C17H, C14H[b]
7	74.90	3.25	$C49H_3$, $C48H_3$, C5H′, C5H″, C6H′, C8H
19	80.60	3.56	$C51H_3$, $C52H_3$, C17H, C18H, C21H
1′	96.00	4.64	C22H
21	122.23	5.16	$C52H_3$, C19H, C22H[c]
39	122.96	5.46	C37H,[c] C38H, C40H′, C40H″, C41H
2	127.01		$C47H_3$, C3H, C4H[c]
12	129.41	5.38	C11H′, C11H″, C14H
16	130.92	5.35	C14H, C15H, C17H
13	132.55	5.38	$C50H_3$, C11H″, C14H
17	132.55	5.44	C51H, C16H, C19H
38	137.44	5.46	C39H,[c] C40H′, C40H″
3	141.81	6.65	$C47H_3$, C4H, C5H′, C5H″
20	143.02		$C52H_3$, C19H, C22H, C18H
1	166.37		$C47H_3$, C3H, C41H

[a] Coupling to one or both of these protons. [b] Connectivity observed in Figure 1 of the supplementary material. [c] Connectivity not observed in Figure 4b but visible at lower contour levels.

Figure 4a between $C51H_3$ and carbons C17 and C18. Protons $C51H_3$ are coupled also to a carbon at 80.6 ppm (C19), which has a directly attached proton at 3.56 ppm. A cross peak in the COSY spectrum between C18H and C19H confirms this. Since the C19H multiplet overlaps with two other protons (sugar protons C5′H and C3′H, vide infra), the HMBC connectivity is essential for determining which carbon resonance corresponds to C19. Methyl protons $C52H_3$ (a singlet at 1.58 ppm) show coupling to carbon C19 (Figure 4a) and to two olefinic carbons at 143.0 and 122.2 ppm (Figure 4b), which then have to correspond to C20 and C21, respectively. C21 has a directly attached proton at 5.16 ppm which is coupled to a proton at 4.17 ppm (C22H) which is coupled to a proton at 3.80 ppm (C23H) (Figure 1). At lower contour levels than shown in Figure 4a (see Figure 1 of the supplementary material) C22H also shows coupling to carbon C21 and to a carbon at 69.5 ppm that is coupled to a proton at 3.80 ppm, confirming the assignment of C23H. C22H shows connectivity to a carbon resonance at 96.0 ppm (outside the region displayed in Figure 4a but present as a folded resonance in Figure 4b), which, as will be shown later, corresponds to C1′ of the mannose sugar ring. The presence of this sugar unit was determined previously by Bognar et al.[2]

Carbons C24 through C29 presented the most difficult part in the structure determination, mainly because of the absence of methyl groups and the severe overlap in the ^1H spectrum. Also, many of the corresponding ^1H multiplets show very broad unresolvable patterns, resulting in very low intensity in the ^1H–^{13}C long-range connectivity spectrum. C22H shows coupling to a carbon at 40.6 ppm (below the lowest contour level in Figure 4a), which cannot be more than three bonds removed from C22H and thus has to be C24. C24 has two directly attached protons resonating at 1.28 ppm, and a cross peak between C23H and $C24H_2$ (Figure 1b) confirms the location of C24. A relay cross peak between C23H and C25H in Figure 2b indicates that C25H resonates at 3.90 ppm, with the corresponding carbon at 63.7 ppm. A weak correlation (below the contour level of Figure 4a but visible in Figure 1 of the supplementary material) between $C24H_2$ and C25 confirms this assignment. In the COSY spectrum (Figure 1b), one finds that C25H shows connectivity to two protons, at 1.28 and 1.43 ppm. The 1.28 ppm resonance corresponds to $C24H_2$, and the 1.43 ppm proton then must be attached to C26. Inspection of the heteronuclear shift correlation spectrum (Figure 3a) indicates that three carbons have an attached proton at 1.43 ppm, the resonances labeled 26, 32, and 34. A priori, it is not clear which of these three resonances is C26. However, the resonance of C34 can be excluded because the HOHAHA spectrum does not show relay from C25H to the other proton (C34H″ at 1.20 ppm) attached to this carbon. As will be shown later, the resonance labeled C32 has a methyl group (C54) attached, and these methyl protons would have to show long-range connectivity to C25 if C32 and C25 were adjacent carbons. Since this connectivity between $C54H_3$ and C25 is not observed, this proves that the resonance at 45.4 ppm must correspond to C26. The expanded display (Figure 2b) of the diagonal region near 3.5 ppm of the HOHAHA spectrum shows relay connectivity between C25H and a proton that is shifted slightly (about 0.02 ppm) upfield from C25H. This proton must correspond to C27H, and additional evidence is found in connectivity between C27 and C26H′ (below the contour level of Figure 4a but visible in Figure 1 of the supplementary material) and between C27 and a proton at 1.51 ppm (C28H″). This latter proton also shows connectivity to C26. C28 is then identified by correlation with C28H″ and C28H′ (C28H′ is found from the expanded region of the COSY spectrum, shown in Figure 1b). C29H (3.61 ppm) is found by HOHAHA correlation with C27H. The C29H multiplet overlaps exactly with the C9H multiplet. Since C9 has been assigned previously, the C29 resonance is identified by inspection of the ^1H–^{13}C shift correlation spectrum (Figure 3b).

The structure of the remaining part of the lactone ring is found relatively straightforwardly, and this part will be discussed in less detail. C29, C30, and C31 are identified on the basis of coupling to protons $C53H_3$. Similarly, C31, C32, and C33 are found by connectivity to protons $C54H_3$. C33H shows J connectivity to C34H′ and C34H″ (Figure 1b) and HOHAHA connectivity to C35H and C37H (Figure 2b). Assignment of the $C36H_2$ protons is based on connectivity with C37H in the COSY spectrum (Figure 1b). C37H shows coupling to an olefinic proton (C38H) at 5.46 ppm. The two remaining unassigned olefinic carbon resonances

(at 137.4 and 123.0 ppm) therefore must correspond to C38 and C39. Figure 3c shows that both C38H and C39H resonate at 5.46 ppm. C39H shows connectivity to two protons at 2.16 (C40H″) and 2.33 ppm (C40H′), which both show connectivity to a proton at 5.05 ppm, which then must be C41H. The inset in Figure 4b shows connectivity between C41H and a carbon at 123.0 ppm, which distinguishes C38 and C39. This inset also shows connectivity between C41H and the carbonyl carbon in the C1 position, which closes the lactone ring and explains the downfield position of the C41H resonance. Methyl $C55H_3$ shows coupling to C41, C42, and C43. C42H shows connectivity to C44, and C43H shows connectivity to C45 (Figure 4a). Finally, the methylene protons at 2.74 ppm ($C46H_2$) show coupling to both C44 and C45. Moreover, C43H shows HOHAHA connectivity to $C46H_2$ (Figure 2a).

Remaining unassigned carbon resonances are all in the 60–75 ppm region and correspond to the mannose sugar unit. Carbon C1′ was assigned on the basis of coupling to C22H. Also, C1′H shows coupling to C22 (Figure 1 of the supplementary material and a folded resonance in Figure 4b), confirming this assignment. C1′H also shows coupling to C2′, C3′, and C5′ (Figure 4a). C2′H is identified from the COSY spectrum and resonates slightly downfield from C3′H, distinguishing C2′ and C3′ in figure 3a. Protons C4′H and C5′H have identical chemical shifts, but assuming the mannose unit is in the pyranoid form (on the basis of the chemical shift of C1′), only C5′ can show long-range connectivity to C1′H. $C6'H_2$ protons can be identified in the COSY spectrum, and they are also attached (Figure 3b) to the only remaining carbon whose resonance was not yet assigned. A subspectrum of all sugar protons is shown as an inset in Figure 2a. This subspectrum represents a F_1 cross section taken at the F_2 frequency of the overlapping C2′H and C3′H resonances.

All resonances in the ^1H and ^{13}C spectrum now have been assigned, and all correlations found in Figures 1–4 are in perfect agreement with the proposed structure. Adding the weights of all protons, carbons, and hydrogens yields a molecular weight of 1175.7307. Our mass spectroscopy indicated a molecular weight of 1192, and previous higher resolution measurements by Dolak et al.[3] indicated a molecular weight of 1191.7402. The difference of 16 units corresponds to an NH_2 that must be attached to C46. The chemical shifts of both $C46H_2$ and C46 are in agreement with the presence of a NH_2 group in this position. Elemental analysis also indicated the presence of nitrogen in the molecule. To prove that the NH_2 is indeed attached to C46, the small amount of water in the sample was removed by repeated lyophilization, allowing detection of the relatively sharp NH_2 resonance at 7.82 ppm. A COSY spectrum (Figure 2 of the supplementary material) then clearly showed J connectivity between this resonance and C46.

The stereochemistry of the olefinic bonds has been determined from measuring ^1H–^1H coupling constants and from 2D NOE data. The C16H–C17H coupling measured from the 1D spectrum is 15.4 Hz, indicating a trans configuration. The couplings between C12H and C13H and between C38H and C39H are measured from Figure 5. For both pairs, a 15.5 ± 1 Hz coupling is found, indicating a trans coupling. We used 2D absorption mode[31] NOE spectroscopy for determining the stereochemistry about the methylated double bonds. The NOE between the methyl protons and the adjacent olefinic proton (Figure 3 of the supplementary material) was very weak (integrated cross-peak volume ≈ 0.3% of integrated diagonal resonance of C3H) for both the C2–C3 and the C20–C21 double bonds, indicating a trans configuration in both cases. Moreover, the NOE data in the supplementary material show substantial NOE's between $C47H_3$ and $C4H_2$ (≈6%) and between C22H and $C52H_3$ (≈8%), confirming these trans configurations.

Materials and Methods

Desertomycin was obtained from Dr. Stephen Bekesi (Biological Institute, Medical University School of Debrecen, Hungary) and was further purified by high-pressure liquid chromatography. For HPLC, a μBondapak C-18 (Waters Associates) column was used in a Waters Model 6000 solvent delivery system and a model 660 solvent programmer (Waters), with a mobile phase of 0.01 N $HCOONH_4$ (pH 7.2) and acetonitrile (7:3), flow rate 1 mL/min. A gradient of acetonitrile was applied over 60 min, to a final composition of 100% acetonitrile. Column output was monitored by UV at 220 nm, and the peak eluting at 21.35 min was collected, precipitated with water (1:1) at 4 °C, filtered, and dried. Purity check: TLC, silica gel GF (Analtech), solvent BuOH–AcOH–H_2O–EtOH (38:10:50:2) upper layer, R_f 0.48, single component. Elemental analysis data were consistent with a molecular formula of $C_{61}H_{109}NO_{21}$.

Mass Spectrometry. The FAB mass spectrum of desertomycin was obtained on a Krator MS-50 double-focusing mass spectrometer (Manchester, U.K.) using a glycerol matrix. A resolving power of 1000 was used in this experiment. The obtained spectrum indicated an $(M + H)^+$ at m/z 1193 and an $(M + Na)^+$ at m/z 1215. When the sample was doped with KCl, an $(M + K)^+$ at m/z 1231 was observed. These data indicate a molecular weight of 1192.

NMR Spectroscopy. All ^1H experiments were recorded on a sample containing 16 mg of desertomycin in 0.4 mL of dimethyl-d_6 sulfoxide. The ^1H–^{13}C shift correlation spectrum of Figure 3 was recorded on a sample containing 120 mg in 3 mL of dimethyl-d_6 sulfoxide. The 2D NOE experiment was carried out at 25 °C; all other experiments were done at 55 °C. Experiments were performed on a modified Nicolet NT-500 spectrometer, equipped with a Cryomagnet Systems[32] probe that has a broad-band decoupling coil outside the ^1H observe coil.

^1H–^1H Correlation Spectroscopy. The double-quantum-filtered COSY spectrum was obtained from a 2 × 450 × 1024 data matrix,[33] which resulted after zero filling in both dimensions in a 1024 × 1024 data matrix for the absorptive part of the 2D spectrum. The spectral width was 2273 Hz in both dimensions; acquisition times were 198 and 225 ms in the t_1 and t_2 dimensions, respectively. The carrier was positioned at 3.06 ppm, and the C3H resonance (at 6.64 ppm) appears as a folded resonance at 1.10 ppm. Exponential line narrowing (3 Hz) was used in both dimensions prior to Fourier transformation. Sixty-four scans were recorded for each t_1 value with a delay time of 2 s between scans. The total measuring time was 16 h.

HOHAHA Spectroscopy. The HOHAHA spectrum resulted from a 2 × 450 × 1024 data matrix, zero filled in both dimensions to yield a 1024 × 1024 data matrix for the absorptive part of the 2D spectrum. The spectral width was 3226 Hz in both dimensions; acquisition times were 140 and 159 ms in the t_1 and t_2 dimensions, respectively. Exponential line narrowing (2 Hz) was used in both dimensions prior to Fourier transformation. A 7.8-kHz radio frequency field strength (5-W radio frequency power) was used (64-μs, 180° pulse width), and the mixing period consisted of 36 MLEV-17 cycles,[12] preceded and followed by 2-ms trim pulses,[12] resulting in a 80-ms mixing time.

^1H–^{13}C Correlation Spectroscopy. The ^1H–^{13}C shift correlation spectrum was recorded in the absorptive mode, using a modified version[18] of the original experiment.[14] The decoupler was positioned in the center of the ^1H spectrum, and the hypercomplex approach[31] was used for distinguishing positive and negative modulation frequencies. The spectrum resulted from a 2 × 170 × 2048 data matrix, zero filled in both dimensions to yield a 256 × 2048 matrix for the absorptive part of the 2D spectrum. Acquisition times were 51 and 57 ms in the t_1 and t_2 dimensions, respectively. Spectral windows were 3333 (t_1) and 17 855 Hz (t_2). For each t_1 value 192 scans were recorded, and the delay time between scans was 1 s; the total measuring time was 11 h. In both dimensions exponential line narrowing (−10 Hz) and Gaussian broadening (+13 Hz) were used prior to Fourier transformation for enhancing the line shape.

Heteronuclear Multiple-Bond Correlation. The recently proposed experiment[19] for detecting long-range ^1H–^{13}C connectivity, utilizing ^1H detection, was used for obtaining the spectra shown in Figure 4. To cover the entire ^{13}C spectral width, two experiments were performed, with the ^{13}C carrier positioned at 54 and 145 ppm, respectively. The spectrum of Figure 4a resulted from a 280 × 1024 data matrix, with 160 scans per t_1 value and an 11.11-kHz F_1 spectral width. The spectrum of Figure 4b resulted from a 210 × 1024 data matrix, with 192 scans per t_1 value and a 7.5-kHz F_1 spectral width. A delay time of 1.4 s (including a 153-ms t_2 acquisition period) was used in both experiments. The total measuring time for each spectrum was about 17 h. Δ_1 and Δ_2 durations in the sequence[19] were 3.4 and 65 ms, respectively, for Figure 4a and 3.0

(31) States, D. J.; Haberkorn, R. A.; Ruben, D. J. *J. Magn. Reson.* **1982**, *48*, 286.

(32) Cryomagnet Systems Inc., 4101 Cashard Ave. No. 103, Indianapolis, IN 46203.

(33) A 2 × 450 × 1024 data matrix indicates that for 450 different t_1 values, two FID's consisting of 1024 data points each (512 complex data points) were acquired and stored in separate locations, as described in ref 31.

and 70 ms for the spectrum of Figure 4b. The ^{13}C 90° pulse width was 100 μs in both experiments.

^{1}H-Detected ^{1}H–^{13}C Correlation. The spectrum of Figure 5 was recorded with the recently published scheme[22] that facilitates suppression of all signals from protons not coupled to ^{13}C by presaturation of these signals by means of a BIRD pulse.[34] No ^{13}C decoupling was employed during ^{1}H data acquisition. The spectrum results from a 2 × 65 × 2048 data matrix, with acquisition times of 16 and 278 ms in the t_1 and t_2 dimensions, respectively. The delay time between scans (including the 278-ms t_2 acquisition period and the 400-ms period between the BIRD pulse and the start of the actual sequence) was 1.28 s. For each t_1 value 128 scans were recorded, and the total measuring time was 3 h. Exponential line narrowing (3 Hz) was used in the t_2 dimension, prior to Fourier transformation; 20-Hz Gaussian broadening was used in the t_1 dimension to avoid truncation artifacts.

Discussion

With the two-dimensional NMR methods discussed above, determination of the structure of molecules of the size and complexity of desertomycin becomes straightforward. The multiple-bond ^{1}H–^{13}C correlation (HMBC) experiment is particularly useful because it utilizes the higher resolution of the ^{13}C spectrum and therefore presents less overlap than ^{1}H–^{1}H correlation methods and because it allows one to bridge heteroatoms and nonprotonated carbons. The experiment yields information somewhat similar to the 2D INADEQUATE experiment.[35] A disadvantage of the HMBC is that the resolution in the F_2 dimension is determined by the resolution in the ^{1}H spectrum, which is usually much lower than that for the INADEQUATE experiment, where the resolution in boht dimensions of the spectrum is governed by ^{13}C spectral dispersion. This disadvantage is more than offset by the gain in sensitivity obtainable in the HMBC experiment. Moreover, the HMBC experiment yields both two- and three-bond ^{1}H–^{13}C connectivity, which is equivalent to the detection of one- and two-bond ^{13}C–^{13}C connectivity. In the INADEQUATE experiment only one-bond connectivities are detected easily, and bridging of heteroatoms is therefore not readily possible. The HMBC experiment is the ^{1}H-detected equivalent of earlier long-range ^{1}H–^{13}C shift correlation experiments.[36,37] The advantage of the HMBC experiment over these earlier experiments lies not only in its higher sensitivity (due to detection of ^{1}H instead of ^{13}C) but also in the fact that the intensity of a correlation in the HMBC experiment reflects more directly the size of the ^{1}H–^{13}C coupling. Because the HMBC experiment requires suppression of signals from protons not coupled to ^{13}C, stability requirements for the spectrometer system are much more demanding than for the older experiments.

All spectra used for the structure determination with the exception of the ^{1}H–^{13}C shift correlation experiment were performed on a 16-mg sample. Most certainly, the ^{1}H–^{13}C correlation experiment also could be determined on this 16-mg sample by using the ^{1}H-detected version of this experiment, HMQC.[22] However, the high-quality spectrum of Figure 3 was recorded before the ^{1}H-detected method was developed, and no attempt was made subsequently to record a high-resolution HMQC spectrum. Therefore, it can be concluded that the newer types of techniques discussed here permit structure determination using relatively small sample quantities.

As deduced from the proposed structure (Chart I), the molecular formula of desertomycin is $C_{61}H_{109}NO_{21}$, corresponding to a molecular weight, $(M + H)^+$, of 1192.7572, in agreement with our mass spectroscopy data (1193) and in excellent agreement with the high-resolution spectrum of Dolak et al.[3] that indicated a $(M + H)^+$ of 1192.7480. The presence of a relatively large lactone ring, suggested earlier by Dolak et al.[3] on the basis of physico-chemical studies, is in agreement with the structure proposed here. Structurally, desertomycin resembles most closely azalomycin[38] and monazomycin.[39]

Acknowledgment. We wish to thank Rolf Tschudin for continuous technical support and Dr. Susanta K. Sarkar for recording some preliminary spectra of desertomycin. We thank Dr. Laura Lerner for many useful comments during the preparation of this manuscript.

Registry No. Desertomycin, 12728-25-5.

Supplementary Material Available: Figure 1 showing a low contour level display of the high-field heteronuclear multiple-bond spectrum, Figure 2 showing an absolute value mode COSY spectrum of desertomycin in dry dimethyl sulfoxide, and Figure 3 showing an absorption mode 2D NOE spectrum of desertomycin (3 pages.) Ordering information is given on any current masthead page.

(34) Garbow, J. R.; Weitekamp, D. P.; Pines, A. *Chem. Phys. Lett.* **1982**, *93*, 504. Bax, A. *J. Magn. Reson.* **1983**, *52*, 330.
(35) Bax, A.; Frenkiel, T.; Freeman, R.; Levitt, M. H. *J. Magn. Reson.* **1981**, *43*, 478.
(36) Bax, A. In *Topics in Carbon-13 NMR*; Levy, G. C., Ed.; Wiley: New York, 1984, Chapter 8.
(37) Kessler, H.; Bermel, W.; Griesinger, C. *J. Am. Chem. Soc.* **1985**, *107*, 1083.
(38) Nakayama, H.; Furikata, K.; Seto, H.; Otake, N. *Tetrahedron Lett.* **1981**, *22*, 5217.
(39) Iwasaki, S.; Namikoshi, M.; Sasaki, K.; Yano, M.; Fukushima, K.; Nozoe, S.; Okuda, S. *Chem. Pharm. Bull.* **1982**, *30*, 1669.